PHYSICAL REVIEW B VOLUME 11, NUMBER 3 1 FEBRUARY 1975

Spin dynamics in multilevel magnetic systems

M. E. Lines
Bell Laboratories, Murray Hill, New Jersey 07974
(Received 4 September 1974)

The correlated-effective-field theory of many-body magnetism, introduced by the author in an earlier paper to describe the equilibrium properties of magnetic ions with complicated level structure, is extended to discuss spin dynamics in a similar context. The method goes beyond the random-phase approximation by incorporating a measure of spontaneous fluctuations in a manner which ensures self-consistency with respect to the fluctuation-dissipation theorem. After a formal derivation of equations defining mode frequency dispersion and scattering strength, the method is used to discuss the problem of singlet-ground-state ferromagnetism. The singlet-triplet model is discussed in the paramagnetic phase and the soft mode on approach to the Curie temperature is shown to be a zone-center zero-frequency electronic mode. A more realistic model involving a singlet-ground-state ion in a cubic-crystal-field environment is also investigated to explore the manner in which excitations between excited crystal-field levels interact with excitations out of the singlet ground state as the temperature is raised. Numerical calculations of frequency dispersion and mode strength are performed as functions of temperature, and quantitative results for the correlated-effective-field and random-phase approximations are compared for both the singlet-triplet and cubic-crystal-field problems.

I. INTRODUCTION

In an earlier paper[1] the present author discussed the difficult many-body problem of describing magnetic systems containing ions of complicated level structure at temperatures for which thermal energies are comparable with exchange energies and crystal-field splittings. Such systems, involving significant thermal population of excited-orbital crystal-field levels, are difficult to treat theoretically except in a local-effective-field approximation. Unfortunately the standard local-field approximation, which is molecular-field theory for equilibrium properties and the random-phase approximation for dynamics, takes no account of spontaneous fluctuations and is therefore numerically very crude in any situation for which cooperative effects are important.

In Ref. 1 we discussed the statics of a self-consistent local-field theory which goes beyond the random phase to incorporate at least some measure of spontaneous fluctuations. This was accomplished by noting that the random-phase approximation violates an important exact relationship (derivable from the fluctuation-dissipation theorem) between static susceptibility and static two-spin, or more exactly two-moment, correlations. By introducing a simple measure of correlations into the definition of a "correlated effective field" it proved possible to determine the latter unequivocally by forcing consistency with the exact fluctuation restraint.

In this paper we shall extend the equilibrium calculation outlined in the earlier paper[1] and discuss spin dynamics in the correlated-effective-field (CEF) approximation. This is accomplished by calculating the linear response of the *correlated* equilibrium configuration to a small time-dependent perturbing magnetic field. The method is to be compared with the "random-phase approximation" (RPA) which describes a linear response of the molecular-field equilibrium configuration.[2] As in Ref. 1, we shall discuss a paramagnetic phase (for which the theory is simpler) but do not wish to imply that the CEF method is incapable of describing an ordered configuration.[3] On the other hand, at low temperatures, for which the equilibrium configuration involves ions which are predominantly in their ground states, conventional spin-wave theory is well defined[4] for describing all excitations from the ground state, and excitations between excited levels are extremely weak.

One set of magnetic problems in which excitations between excited levels play an important role, and for which the conventional molecular-field RPA hybrid theoretical approximation has been used with less than wholly satisfying results, is that of the rare-earth singlet-ground-state ferromagnets.[5-18] For a recent review see Birgeneau.[17] In particular, controversy surrounds the question of the character of the soft mode in these systems and there is poor agreement between RPA theory and the temperature dependence of the magnetic excitations. Although the dynamic theory as developed in this paper will not be restricted to singlet-ground-state situations, we shall cast it in the conventional rare-earth symbolism in order to facilitate an examination of the singlet-ground-state problem as a simple numerical application in the later sections. We shall establish, for example, that the soft mode in the singlet-triplet model is the zero-frequency electronic triplet-triplet excitation at long wavelengths. We shall also compare numerically the CEF and RPA

dispersion and mode-strength relations and their temperature development for the full cubic level excitations in a more realistic structural situation.

II. STATIC THEORY

Before studying dynamic linear response in the CEF approximation we shall first outline the concept of the correlated effective field and restate the basic defining equations of static CEF theory in the new notation. Let us consider a many-body Hamiltonian

$$\mathcal{H}=\sum_i V_{ci}-2\sum_{i>j}\mathcal{J}_{ij}\vec{\mathbf{J}}_i\cdot\vec{\mathbf{J}}_j-\sum_i g_J\mu_B H_i J_i^z, \quad (2.1)$$

in which V_{ci} is a crystal-field operator at the ith magnetic site, $\mathcal{J}_{ij}$ an exchange parameter, $\vec{\mathbf{J}}_i$ an angular momentum operator with J_i^z its z component, and H_i an applied field in the z direction. In contrast to the more general situation described in Ref. 1, in which we allowed for a more general bilinear exchange formalism and a crystal-field operator of arbitrary complexity, we have here adopted an isotropic exchange form and shall later assume V_{ci} to be of sufficiently high symmetry to produce an isotropic magnetic susceptibility (e.g., cubic). This allows for considerable simplification of the formalism while still enabling us to discuss the fundamental difference of RPA and CEF and the basic problems of singlet-ground-state ferromagnetism alluded to in Sec. I. Generalization to an anisotropic situation is formally quite straightforward.

The equation of motion for angular momentum $\vec{\mathbf{J}}_i$ in the absence of applied field H_i is

$$\dot{J}_i^x=\frac{i}{\hbar}[V_{ci},J_i^x]_- -2\sum_j\mathcal{J}_{ij}(J_i^zJ_j^y-J_i^yJ_j^z), \quad (2.2)$$

where $[\ ,\ ]_-$ is a commutator, together with the two equations resulting from the cyclic permutation of x,y,z. In RPA this set of equations is closed by approximating all jth-site operators by their ensemble averages. In CEF[1] we write (2.2) as

$$\dot{J}_i^x=(i/\hbar)[V_{ci},J_i^x]_- -J_i^z h_{\mathrm{corr}}^y+J_i^y h_{\mathrm{corr}}^z, \quad (2.3)$$

introducing components h_{corr}^γ ($\gamma=x,y,z$) of a *correlated* effective field defined by

$$h_{\mathrm{corr}}^\gamma=2\sum_j\mathcal{J}_{ij}[\langle J_j^\gamma\rangle+\alpha^\gamma(J_i^\gamma-\langle J_i^\gamma\rangle)], \quad (2.4)$$

where α^γ are temperature-dependent correlation parameters. In this manner the many-body problem is reduced to noninteracting form [i.e., Eq. (2.3) now involves ith-site operators only]. In the absence of applied field H_i the ensemble averages in (2.4) vanish and, after properly symmetrizing to render the observable $\dot{J}_i^x$ Hermitian, we find the CEF equation of motion

$$\dot{J}_i^x=(i/\hbar)[V_{ci},J_i^x]_- -\sum_j\mathcal{J}_{ij}(\alpha^y-\alpha^z)(J_i^yJ_i^z+J_i^zJ_i^y), \quad (2.5)$$

together with the cyclic permutations. This set of equations of motion can be obtained in a formal manner from an effective ith-site Hamiltonian

$$\mathcal{H}_i^0(\mathrm{eff})=V_{ci}-\sum_j\sum_\gamma\mathcal{J}_{ij}\alpha^\gamma(J_i^\gamma)^2. \quad (2.6)$$

Solving for the eigenstates $|n\rangle$ and eigenvalues E_n of (2.6), the static susceptibility can then be derived as a function of α^γ by including an infinitesimal magnetic-field energy in the effective Hamiltonian (2.6) and using perturbation theory. The resulting susceptibility $\chi^\gamma(\vec{\mathbf{q}})$, where $\vec{\mathbf{q}}$ is a wave vector, is directly related to static-moment correlations via the fluctuation relation[1]

$$\sum_{\vec{\mathbf{q}}}\chi^\gamma(\vec{\mathbf{q}})=Ng_J^2\mu_B^2\left\langle\int_0^{1/kT}e^{\theta\mathcal{H}_i^0(\mathrm{eff})}\times J_i^\gamma e^{-\theta\mathcal{H}_i^0(\mathrm{eff})}J_i^\gamma d\theta\right\rangle_0, \quad (2.7)$$

where there are N magnetic atoms in the macroscopic lattice and where the ensemble average $\langle\cdots\rangle_0$ is with respect to the zero-field ensemble defined by (2.6). Equation (2.7) determines the correlation parameters α^γ completely in the form[1]

$$\alpha^\gamma=\sum_{\vec{\mathbf{q}}}\eta^\gamma(\vec{\mathbf{q}})\mathcal{J}(\vec{\mathbf{q}})\Big/\sum_{\vec{\mathbf{q}}}\eta^\gamma(\vec{\mathbf{q}})\,\mathcal{J}(0), \quad (2.8)$$

in which

$$[\eta^\gamma(\vec{\mathbf{q}})]^{-1}=kT-2[\mathcal{J}(\vec{\mathbf{q}})-\alpha^\gamma\mathcal{J}(0)]\langle J^\gamma:J^\gamma\rangle_0, \quad (2.9)$$

where $\mathcal{J}(\vec{\mathbf{q}})$ is the Fourier transform with respect to the lattice of the exchange $\mathcal{J}_{ij}$ and

$$\langle J^\gamma:J^\gamma\rangle_0=\sum_n\rho_n\left(J_{nn}^\gamma J_{nn}^\gamma+2kT\sum_{m\neq n}\frac{J_{nm}^\gamma J_{mn}^\gamma}{E_m-E_n}\right), \quad (2.10)$$

where ρ_n is the density matrix

$$e^{-E_n/kT}\Big/\sum_n e^{-E_n/kT},$$

E_n are the eigenvalues of the effective Hamiltonian (2.6), and J_{nm}^γ is the matrix element $\langle n|J^\gamma|m\rangle$.

In a general anisotropic V_{ci} environment, Eq. (2.8) defines three equations to be solved simultaneously for the three correlation parameters α^x, α^y, α^z, where directions x, y, z, diagonalize the susceptibility. The simplifications resulting from a high-symmetry crystal field V_{ci} (such as cubic) are twofold. First, since $\alpha^x=\alpha^y=\alpha^z=\alpha$ by symmetry, the self-consistency condition (2.8) reduces to a single implicit equation for correlation α. Even more importantly, from a computational point of view, the last term in (2.6) now becomes equal to a constant $\alpha J(J+1)\sum_j\mathcal{J}_{ij}$ and can therefore be dropped from statistical calculation. The eigenstates $|n\rangle$ and eigenvalues E_n are therefore independent of correlations in this high-symmetry situation and are

just the eigenstates and eigenvalues of V_{ci}. The self-consistency condition (2.8) is correspondingly simplified still further.

III. DYNAMIC LINEAR RESPONSE

In the presence of a perturbing field $H_i^z e^{-i\omega t}$ the ensemble averages in (2.3), (2.4) are no longer zero and the resulting effective Hamiltonian for the ith site becomes

$$\mathcal{H}_i(\text{eff}) = V_{ci} - \sum_j \sum_\gamma \alpha \mathcal{J}_{ij} (J_i^\gamma)^2 - g_J \mu_B J_i^z H_i^z e^{-i\omega t} - 2\sum_j \mathcal{J}_{ij} J_i^z (\langle J_j^z \rangle - \alpha \langle J_i^z \rangle), \tag{3.1}$$

where we have used the symmetry condition $\alpha^\gamma = \alpha$, and the second term on the right-hand side is just a constant. The perturbing field at the ith site is therefore

$$H_i(\text{eff}) = H_i^z e^{-i\omega t} + \frac{2}{g_J \mu_B} \sum_j \mathcal{J}_{ij} (\langle J_j^z \rangle - \alpha \langle J_i^z \rangle). \tag{3.2}$$

We now define a linear response

$$N g_J \mu_B \langle J_i^z \rangle = \varphi(\omega) H_i(\text{eff}), \tag{3.3}$$

where $\varphi(\omega)$ is the dynamic response or susceptibility in the noninteracting limit of zero exchange. Fourier transforming with respect to the lattice we now define a many-body dynamic susceptibility

$$\chi(\vec{q}, \omega) = N g_J \mu_B \langle J(\vec{q}) \rangle / H^z(\vec{q}) e^{-i\omega t} = N g_J^2 \mu_B^2 \varphi(\omega) \{ N g_J^2 \mu_B^2 - 2\varphi(\omega)[\mathcal{J}(\vec{q}) - \alpha \mathcal{J}(0)] \}^{-1}, \tag{3.4}$$

where we omit any component notation on susceptibility because of the isotropy condition.

Defining a time-dependent zz correlation function $\langle [J_i^z(t), J_j^z(0)]_+ \rangle$, where $[\ ,\ ]_+$ is an anticommutator, its Fourier transform with respect to both lattice and time $S^+(q, \omega)$ is directly related to the dynamic susceptibility via the fluctuation-dissipation theorem[19]

$$N g_J^2 \mu_B^2 S^+(\vec{q}, \omega) = \pi^{-1} \coth(\omega / 2kT)\ \text{Im}\chi(\vec{q}, \omega), \tag{3.5}$$

where Im defines the imaginary part. For the noninteracting case of zero exchange, the Heisenberg operators $J_i^z(t)$ and $J_j^z(0)$ are independent and the zz time-dependent correlation function can be written exactly in terms of the matrix elements $J_{nm}^z = \langle n | J^z | m \rangle$, where $|m\rangle$ and $|n\rangle$ are the crystal-field eigenstates of the isolated magnetic ion. By direct calculation we find

$$S_{\text{NI}}^+(\vec{q}, \omega) = \sum_n \rho_n \sum_m |J_{nm}^z|^2 [\delta(E_{nm} - \omega) + \delta(E_{nm} + \omega)], \tag{3.6}$$

in which the subscript NI stands for noninteracting, ρ_n is the density matrix, and $E_{nm} = E_n - E_m$. The corresponding dynamic susceptibility follows from the fluctuation form[20]

$$\chi(\vec{q}, \omega) = N g_J^2 \mu_B^2 \lim_{\epsilon \to 0} \int_{-\infty}^{\infty} \tanh(E/2kT) \times S^+(\vec{q}, E)(E - \omega - i\epsilon)^{-1}\, dE, \tag{3.7}$$

and for the noninteracting limit, using (3.6), gives

$$\chi_{\text{NI}}(\vec{q}, \omega) = \varphi(\omega) = N g_J^2 \mu_B^2 \sum_n \rho_n \sum_m |J_{nm}^z|^2 \times \frac{2E_{nm}}{E_{nm}^2 - \omega^2} \tanh \frac{E_{nm}}{2kT}. \tag{3.8}$$

With an explicit form for $\varphi(\omega)$ we can now use (3.4) to calculate the dynamic susceptibility in the correlated effective-field approximation for the interacting-ion problem. Retaining the infinitesimal in (3.7), Eq. (3.8) is more exactly written as

$$\varphi(\omega) = N g_J^2 \mu_B^2 (R + iP), \tag{3.9}$$

in which

$$R = \sum_n \rho_n \sum_m |J_{nm}^z|^2 \tanh \frac{E_{nm}}{2kT} \times \left(\frac{E_{nm} - \omega}{(E_{nm} - \omega)^2 + \epsilon^2} + \frac{E_{nm} + \omega}{(E_{nm} + \omega)^2 + \epsilon^2} \right), \tag{3.10}$$

and

$$P = \pi \sum_n \rho_n \sum_m |J_{nm}^z|^2 \tanh \frac{E_{nm}}{2kT} \times [\delta(E_{nm} - \omega) - \delta(E_{nm} + \omega)], \tag{3.11}$$

where the δ function $\delta(x)$ is defined by

$$\delta(x) = \lim_{\epsilon \to 0} \frac{\pi^{-1}\epsilon}{x^2 + \epsilon^2}. \tag{3.12}$$

Substituting (3.9) into (3.4) and using (3.5), we find

$$S^+(\vec{q}, \omega) = \pi^{-1} \coth(\omega / 2kT) \times \{P / [(1 - 2\mathcal{J}_\alpha R)^2 + (2\mathcal{J}_\alpha P)^2]\}, \tag{3.13}$$

for the scattering function of the interacting problem, where

$$\mathcal{J}_\alpha = \mathcal{J}(\vec{q}) - \alpha \mathcal{J}(0). \tag{3.14}$$

Now P is the sum of δ-function contributions and it therefore follows that $S^+(\vec{q}, \omega)$ is zero except when

$$2\mathcal{J}_\alpha R = 1. \tag{3.15}$$

Written explicitly this is

$$2[\mathcal{J}(\vec{q}) - \alpha \mathcal{J}(0)] \sum_n \rho_n \sum_m |J_{nm}^z|^2 \times \left(\tanh \frac{E_{nm}}{2kT} \right) \frac{2E_{nm}}{E_{nm}^2 - \omega^2} = 1, \tag{3.16}$$

with solutions $\omega = \omega(\vec{q})$, which define the propagating excitation frequencies of the many-body problem in CEF approximation. The mode strengths follow

directly from (3.13) as

$$S^{+}(\vec{q},\omega)=\sum_{\omega(\vec{q})}\left(\coth\frac{\omega(\vec{q})}{2kT}\right)\frac{\delta(\omega-\omega(\vec{q}))}{4A[\mathcal{J}(\vec{q})-\alpha\mathcal{J}(0)]^2}, \quad (3.17)$$

in which

$$A=\sum_n\rho_n\sum_m|J^z_{nm}|^2\frac{4E_{nm}\omega(\vec{q})}{[E^2_{nm}-\omega^2(\vec{q})]^2}\tanh\frac{E_{nm}}{2kT}. \quad (3.18)$$

The CEF approximation therefore defines many-body excitations of infinite lifetime with dispersion relations $\omega=\omega(\vec{q})$ given by the solutions of (3.16) and with strengths $S(\vec{q},\omega(\vec{q}))$ according to 3.17. The correlation parameter α in these equations is derived as a function of temperature from (2.8). The results have been derived for a system with isotropic susceptibility but within this restriction can immediately be applied to energy-level schemes of arbitrary complexity. The equivalent random-phase results are obtained by putting the correlation parameter equal to zero. Apart from its increased numerical accuracy, one great advantage of the CEF over RPA is that it obeys sum rules of the type

$$\int_{-\infty}^{\infty}\sum_{\vec{q}}S^{+}(\vec{q},\omega)\,d\omega=2N\langle(J^z)^2\rangle, \quad (3.19)$$

and hence allows for self-consistency checks to be carried out during difficult numerical computations.

IV. SINGLET-TRIPLET FERROMAGNET

One problem which is immediately open to attack by the above formalism is the singlet-triplet model for a singlet ground-state ferromagnet.[17] The defining Hamiltonian is (2.1) where now the crystal-field operator V_{ci} is assumed to have a ground singlet eigenstate $|G,0\rangle$ and a triplet excited eigenstate $|E,1\rangle$, $|E,0\rangle$, $|E,-1\rangle$ at an energy Δ higher. The nonzero elements of angular momentum within and between these states are

$$\begin{aligned}&\langle G,0|J^z|E,0\rangle=\langle E,0|J^z|G,0\rangle=M_1,\\&\langle E,\pm1|J^z|E,\pm1\rangle=\pm M_2,\end{aligned} \quad (4.1)$$

with similar expressions for J^{+} and J^{-}. For very small values of $\mathcal{J}(0)/\Delta$ the system remains a paramagnet down to absolute zero. Above a critical value of this ratio, however, it undergoes a phase transition at a Curie temperature T_C to an isotropic ferromagnetic phase.[17]

One of the major controversies surrounding the model is the nature of the soft mode at the Curie point. Published mean-field RPA calculations suggest that the singlet-triplet mode does not go to zero frequency at the transition for any wave vector. On the other hand, the isotropic nature of the ordered phase implies the existence of a long-wavelength zero-frequency (Goldstone) mode corresponding to the rotation of the magnetic moment. Smith[15] has pointed out that an intratriplet (electronic) zero-frequency mode also has the correct group-theoretical representation to be the soft mode and should, at very least, be included self-consistently in the dynamics of a satisfactory theoretical representation of the phase transition.

Let us consider the CEF equations for this particular singlet-triplet model in the paramagnetic phase for which the symmetry restriction imposed in Sec. III is valid. We may then study the phase transition by approaching it from the high-temperature side $T\to T_C^{+}$. First we use the result for uniform static susceptibility in the CEF approximation [Eq. (3.15) of Ref. 1] which, in the present notation, simplifies to

$$\chi(\vec{q}=0)=\frac{g_J^2\mu_B^2\langle J^z:J^z\rangle_0}{kT-2\mathcal{J}(0)(1-\alpha)\langle J^z:J^z\rangle_0}, \quad (4.2)$$

where $\langle J^z:J^z\rangle_0$ has been defined in (2.10). It diverges at the Curie temperature

$$kT_C=2\mathcal{J}(0)(1-\alpha_C)\langle J^z:J^z\rangle_{0,c}, \quad (4.3)$$

where the subscript c refers to values calculated at the transition temeprature. For the singlet-triplet model we find

$$\langle J^z:J^z\rangle_0=(2kTM_1^2/\Delta)F_1+2M_2^2F_2, \quad (4.4)$$

in which

$$F_1=(x-1)/(x+3),\quad F_2=1/(x+3),\quad x=e^{\Delta/kT}. \quad (4.5)$$

Using (4.4) in (4.3), the Curie temperature for the singlet-triplet model is

$$kT_C=4\mathcal{J}(0)(1-\alpha_C)[(kT_CM_1^2F_{1,c}/\Delta)+M_2^2F_{2,c}]. \quad (4.6)$$

The correlation parameter α_c is given by (2.8) as

$$\alpha_C=\frac{\sum_{\vec{q}}\mathcal{J}(\vec{q})/\{kT_C-2[\mathcal{J}(\vec{q})-\alpha_C\mathcal{J}(0)]\langle J^z:J^z\rangle_{0,c}\}}{\sum_{\vec{q}}\mathcal{J}(0)/\{kT_C-2[\mathcal{J}(\vec{q})-\alpha_C\mathcal{J}(0)]\langle J^z:J^z\rangle_{0,c}\}}, \quad (4.7)$$

which, using (4.3), simplifies to

$$\alpha_C=\frac{\sum_{\vec{q}}\mathcal{J}(\vec{q})/[\mathcal{J}(0)-\mathcal{J}(\vec{q})]}{\sum_{\vec{q}}\mathcal{J}(0)/[\mathcal{J}(0)-\mathcal{J}(\vec{q})]}, \quad (4.8)$$

a value which is *independent* of the level structure and depends only on the topology of the lattice. Thus, contrary to earlier suggestions in the literature, there is (at least within the CEF approximation) nothing anomalous about the static correlations near a singlet-triplet transition. The values $\alpha_C=0.256$, 0.282, 0.341 for the nearest-neighbor exchange fcc, bcc, and sc lattices, respectively, are exactly those which would be predicted within the CEF approximation for the equivalent simple Heisenberg models. This equivalence, however, does not extend to temperatures other than $T=T_C$.

The dynamics of the singlet-triplet model, and in particular the role played by the intratriplet modes,

is most easily seen by choosing a new set of quasi-degenerate triplet states as follows: $(2)^{-1/2}(|E,+1\rangle + |E,-1\rangle)$, $|E,0\rangle$, $(2)^{-1/2}(|E,+1\rangle - |E,-1\rangle)$, with energies $\Delta+\frac{1}{2}\epsilon$, Δ, $\Delta-\frac{1}{2}\epsilon$, respectively, and taking the limit $\epsilon \to 0$. Equation (3.16) for the many-body eigenfrequencies now becomes

$$kT = 4[\mathcal{J}(\vec{q}) - \alpha\mathcal{J}(0)] \times [kTM_1^2F_1\Delta/(\Delta^2-\omega^2) + M_2^2F_2\epsilon^2/(\epsilon^2-\omega^2)]. \quad (4.9)$$

As $\epsilon \to 0$ this equation always has a solution $\omega = \lambda(\vec{q})\epsilon$, where

$$kT = 4[\mathcal{J}(\vec{q}) - \alpha\mathcal{J}(0)]\{kTM_1^2F_1/\Delta + M_2^2F_2/[1-\lambda^2(\vec{q})]\}. \quad (4.10)$$

On comparison with Eq. (4.6) for Curie temperature, it is immediately evident that $\lambda(\vec{q}) \to 0$ as $T \to T_C$ and $\vec{q} \to 0$. Thus, even for a finite (but small) value of ϵ the long-wavelength intratriplet (electronic) mode would go soft on approach to the Curie point. This suggests that the long-wavelength electronic mode is the true soft mode. We shall confirm it below by calculating its mode strength. But first let us locate the singlet-triplet mode. Neglecting terms of order of smallness ϵ^2 one easily verifies that (4.9) has a second solution

$$\omega^2 = \omega_H^2(\vec{q}) = \Delta^2 - 4M_1^2F_1\Delta[\mathcal{J}(\vec{q}) - \alpha\mathcal{J}(0)], \quad (4.11)$$

corresponding to just such a mode. At T_C this mode has a minimum value at $\vec{q}=0$ given by

$$\omega_H^2(\vec{q}=0) = 4\mathcal{J}(0)(1-\alpha_C)M_2^2F_{2,c}\Delta^2/kT_C, \quad (4.12)$$

which is nonzero if M_2 and Δ are nonzero. This singlet-triplet mode therefore remains "hard" at T_C and we label it with a subscript H to denote this fact. Accordingly, we shall label the zero-frequency branch $\omega = \omega_S(\vec{q}) = \lambda(\vec{q})\epsilon$ with a subscript S denoting the soft mode.

Using (3.17) it is now simple to calculate the relevant mode strengths $S(\vec{q},\omega(\vec{q}))$ where

$$S^+(\vec{q},\omega) = \sum_{\pm\omega(q)} S(\vec{q},\omega(\vec{q}))\delta(\omega-\omega(\vec{q})), \quad (4.13)$$

where $\omega(\vec{q})$ runs over the two values $\omega_S(\vec{q})$ and $\omega_H(\vec{q})$. We find

$$S_H(\vec{q}) \equiv S(\vec{q},\omega_H(\vec{q})) = [\Delta M_1^2F_1/\omega_H(\vec{q})]\coth[\omega_H(\vec{q})/2kT] \quad (4.14)$$

and

$$S_S(\vec{q}) \equiv S(\vec{q},\omega_S(\vec{q})) = 2M_2^2F_2\Delta^2/[\lambda^2(\vec{q})\omega_H^2(\vec{q})]. \quad (4.15)$$

We note two important points as follows: (a) $S_S(\vec{q})$ is independent of ϵ in lowest order and (b) $S_S(\vec{q})$ diverges as $\lambda(\vec{q}) \to 0$, which is as $T \to T_C$ and $q \to 0$. Eliminating $\lambda(\vec{q})$ from (4.15) by using (4.10), the precise manner in which this divergence takes place may be examined. For example, at the Curie point itself, we find a divergence at long wavelengths of the form

$$S_S(\vec{q}) = kT_C/2bq^2\mathcal{J}(0), \quad (4.16)$$

where we have defined $\mathcal{J}(0) - \mathcal{J}(\vec{q}) = bq^2\mathcal{J}(0)$ as $q \to 0$. This divergence of the triplet-triplet mode strength at T_C confirms our identification of the soft mode as the infinite-wavelength electronic mode.

In order to make the picture clearer and to assess the quantitative and qualitative differences between CEF and RPA we have performed some numerical computations in both approximations for the case $kT_C/\Delta = 1$ and $M_1 = M_2 = M$, assuming nearest-neighbor exchange only and a simple-cubic lattice. In Figs. 1 and 2 we compare the CEF and RPA predictions for the hard mode in cubic-axis and body-diagonal dispersion directions. We note first that

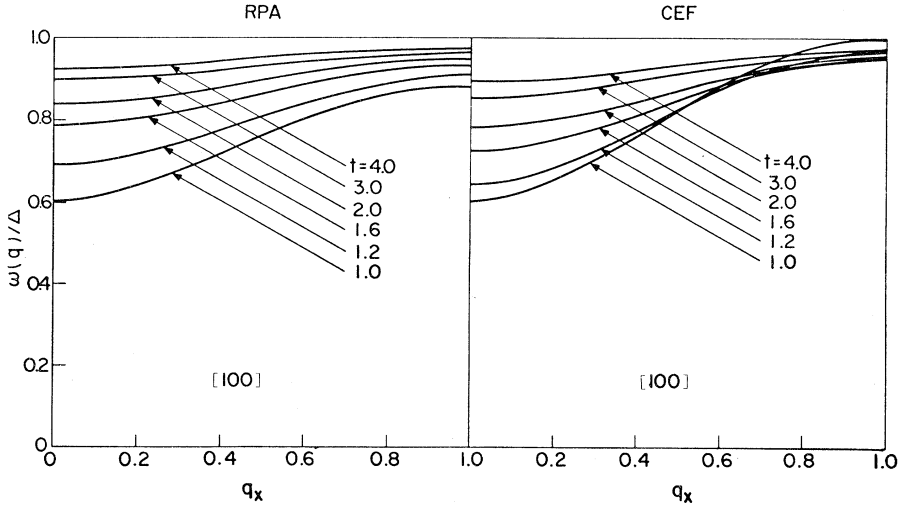

FIG. 1. Dispersion of the singlet-triplet "hard" mode in a [100] direction is calculated for a simple-cubic singlet-ground-state ferromagnet with $kT_C = \Delta$ at several values of temperature $t = kT/\Delta \geq 1$ and the results of RPA and CEF calculations compared. The wave vector q is measured in units of π/a, where a is the linear dimension of the simple-cubic unit cell in real space.

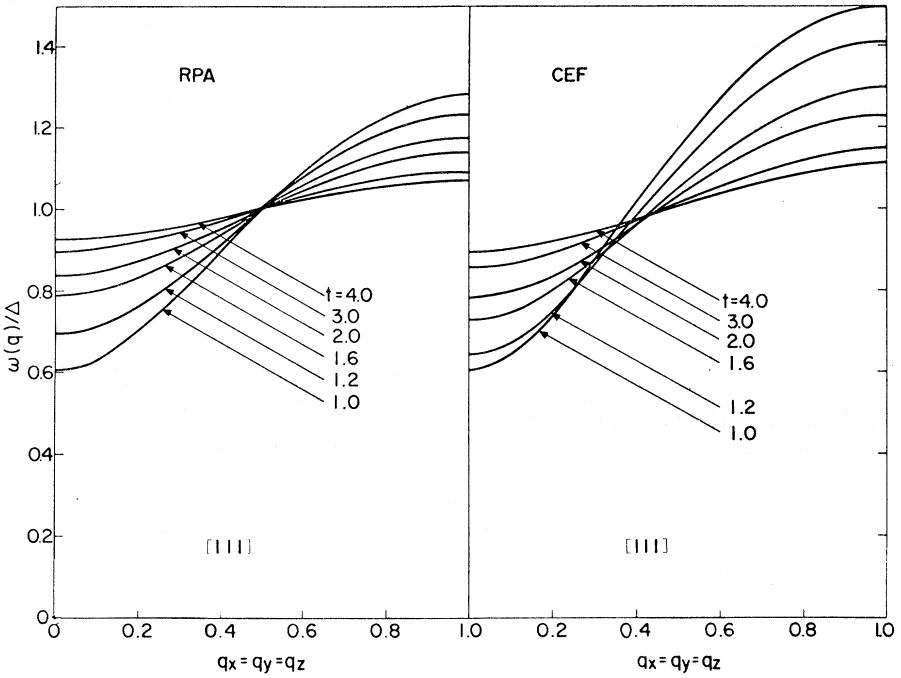

FIG. 2. As Fig. 1, but for dispersion measured along a [111] direction.

the model is defined as having $kT_C = \Delta$ which requires different values of exchange in RPA and CEF. Since $\alpha_C = 0.341$ in CEF and zero in RPA we find from (4.6) that $\mathcal{J}(0)_{\mathrm{CEF}} = 1.516\ \mathcal{J}(0)_{\mathrm{RPA}}$. More specifically, we have

$$\mathcal{J}(0) = \Delta/[1.901\, M^2(1-\alpha_C)] \qquad (4.17)$$

for our case. Comparing the shapes of the dispersion curves we note that the monotonic decrease of [100] curves with decreasing temperature predicted by RPA does not hold in CEF. Another significant feature of the RPA curves, the temperature independence of the $\vec{q} = (\frac{1}{2}\frac{1}{2}\frac{1}{2})$ hard mode, is also not present in CEF. Quantitatively the CEF modes acquire larger dispersions as the temperature is lowered but the zone-center energy gap at $T = T_C$ is the same ($\sim 0.607\Delta$) in both schemes.

The correlation parameter as a function of temperature is plotted in Fig. 3 for the CEF approximation; it increases steadily as the Curie temperature is approached. For the present case of nearest-neighbor exchange it is not difficult to establish from its definition that α is a measure of nearest-neighbor correlations in the form

$$\alpha = \langle J_i^z J_j^z \rangle / [\tfrac{1}{3} J(J+1)]\ , \qquad (4.18)$$

where i and j are nearest-neighbor sites.

Finally, the soft- and hard-mode strengths for [100] dispersion branches are shown for RPA and CEF approximations in Figs. 4 and 5, respectively. In both approximations the divergence of the long-wavelength electronic mode is evident while no anomaly is observed for hard-mode (i.e., singlet-triplet) strength at any wavelength or temperature. It is apparent that the qualitative character of the soft mode can be described in both approximations. Quantitatively, however, only CEF is self-consistent with respect to the fluctuation theorem and we

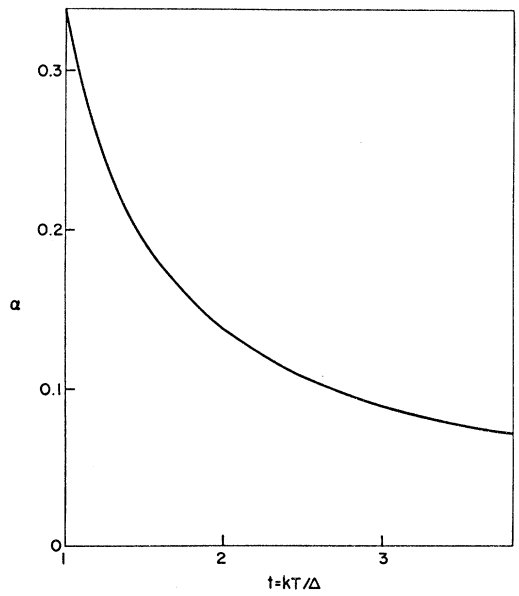

FIG. 3. CEF correlation parameter α is shown as a function of temperature $t = kT/\Delta$ above the Curie temperature $t = 1$ ($\alpha = 0$ in RPA).

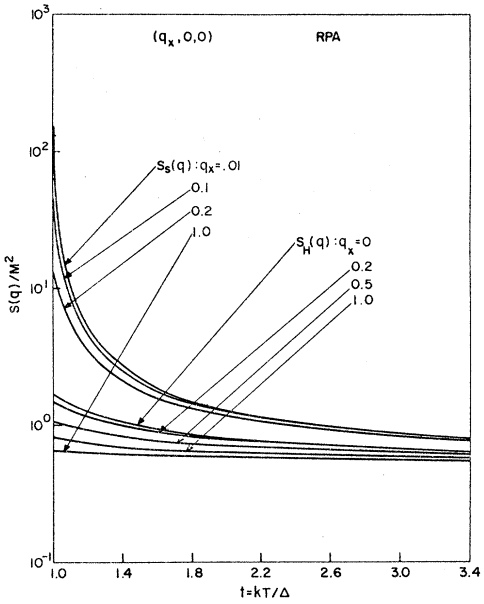

FIG. 4. Mode strengths $S_H(\vec{q})$ and $S_S(\vec{q})$ from the singlet-triplet (hard) and zero-frequency electronic (soft) modes, respectively, are plotted as functions of temperature $t=kT/\Delta$ for several values of wave vector along a [100] direction using the RPA approximation. Wave vector is again measured in units of π/a.

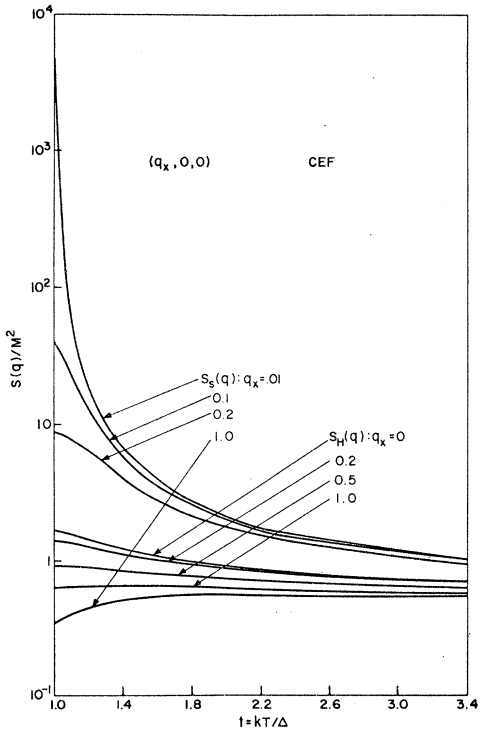

FIG. 5. As Fig. 4, but with calculations performed in the CEF approximation.

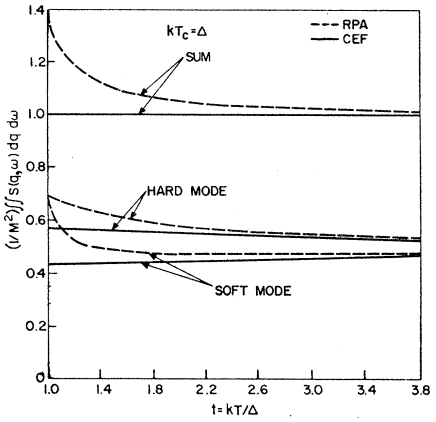

FIG. 6. Separate contributions of hard- and soft-mode strengths to the sum rule (4.20) are computed in RPA and CEF approximations together with their sum. The violation of this fluctuation sum rule by the RPA approximation and its validity in CEF theory are clearly displaved.

can demonstrate this fact numerically by performing the summation over the Brillouin zone appearing in the fluctuation sum rule (3.19). For the singlet-triplet model (3.19) reduces to

$$\sum_{\vec{q}}[S_H(\vec{q})+S_S(\vec{q})]=N\langle(J^z)^2\rangle, \tag{4.19}$$

where we have performed the δ-function integrations over frequency dictated by (4.13). For our particular numerical model with equal matrix elements $M_1=M_2=M$ one obtains directly from (4.1) the result that the operator $(J^z)^2$ is a constant equal to M^2. Thus, sum rule (3.19) for our particular case becomes

$$M^{-2}\langle S_H(\vec{q})+S_S(\vec{q})\rangle_{BZ}=1, \tag{4.20}$$

where $\langle\cdots\rangle_{BZ}$ implies an average over the Brillouin zone. Computing this sum numerically within both RPA and CEF, we obtain the results shown in Fig. 6 where we display separately the contributions from the soft and hard modes as well as their sum. We see that the sum rule is indeed satisfied by CEF but is increasingly violated by RPA as the temperature is lowered towards the Curie point $kT_C=\Delta$. In addition to providing a check on the numerical computation, the CEF verification of the fluctuation sum rule confirms the validity of treating the electronic triplet as the $\epsilon\to 0$ limit of a triplet with an initial infinitesimal splitting ϵ.

V. CUBIC-CRYSTAL-FIELD ENVIRONMENT

The isotropic singlet-triplet model is often used to approximate the more complicated electronic level scheme found in cubic rare-earth singlet-ground-state ferromagnets. Thus, for example, the crystal-field level schemes for Tm^{3+} and Tb^{3+} $(J=6)$ and

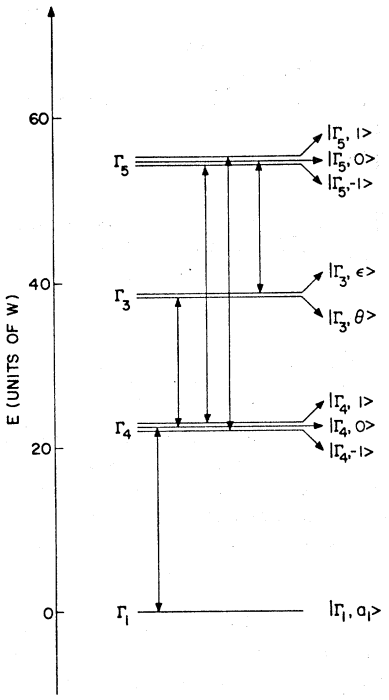

FIG. 7. Energy levels of a $J=4$ magnetic ion in a point-charge face-centered-cubic environment. The arrows indicate the nonzero values of matrix elements of J^z between the states.

for Pr^{3+} ($J=4$) in cubic environment typically have Γ_1 singlet lowest and Γ_4 triplet as first excited level, giving as a first approximation a singlet-triplet model. The additional electronic levels at higher energies are nevertheless not without important effects, particularly at higher temperatures, and indeed Holden and Buyers[21] (using the RPA approximation) have explained an observed lack of Γ_1-Γ_4-mode softening in Pr_3Tl, as observed by neutrons, by an interaction between the Γ_1-Γ_4 mode and a thermally populated Γ_4-Γ_3 excitation.

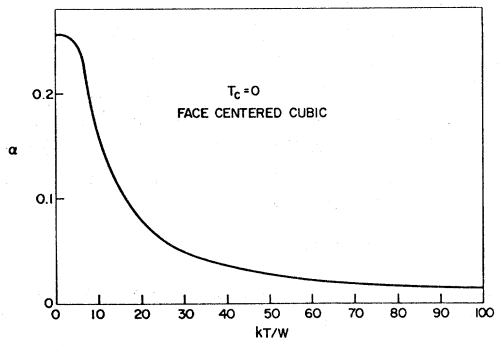

FIG. 8. CEF correlation parameter α as a function of temperature kT/W for the $T_C=0$, $J=4$ face-centered-cubic singlet-ground-state ferromagnet.

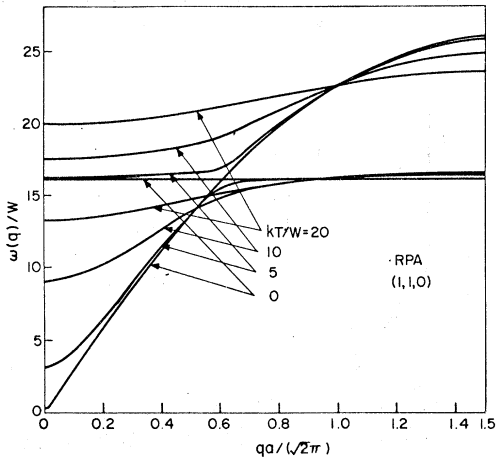

FIG. 9. Dispersion, along a [110] direction in the first fcc Brillouin zone, of the lowest two finite-frequency modes for several values of temperature kT/W as calculated in RPA.

It is an advantage of the CEF method as outlined in this paper that the full cubic-level problem is in principle no more difficult to pursue than the singlet-triplet model. Let us consider specifically a cubic V_{ci} in (2.1) and $J=4$. In a cubic crystal field the eigenstates are completely determined by symmetry and the eigenvalues E are also determined to within an amplitude factor W and a parameter x measuring the ratio of fourth- to sixth-order anisotropy.[13] Explicitly for $J=4$ the symmetry, energy and eigenfunctions are

$$\Gamma_1,\quad E=(-80-52x)W,$$
$$|\Gamma_1,a_1\rangle = 7^{1/2}3^{-1/2}2^{-1}|0\rangle + 5^{1/2}6^{-1/2}2^{-1}(|4\rangle + |-4\rangle); \tag{5.1}$$

$$\Gamma_3,\quad E=(64+68x)W,$$
$$|\Gamma_3,\theta\rangle = 7^{1/2}6^{-1/2}2^{-1}(|4\rangle + |-4\rangle) - 5^{1/2}3^{-1/2}2^{-1}|0\rangle,$$
$$|\Gamma_3,\epsilon\rangle = 2^{-1/2}|2\rangle + 2^{-1/2}|-2\rangle; \tag{5.2}$$

$$\Gamma_4,\quad E=(4+18x)W,$$
$$|\Gamma_4,1\rangle = 2^{-1/2}2^{-1}|-3\rangle + 7^{1/2}2^{-1/2}2^{-1}|1\rangle,$$
$$|\Gamma_4,0\rangle = 2^{-1/2}|4\rangle - 2^{-1/2}|-4\rangle,$$
$$|\Gamma_4,-1\rangle = 2^{-1/2}2^{-1}|3\rangle + 7^{1/2}2^{-1/2}2^{-1}|-1\rangle \tag{5.3}$$

$$\Gamma_5,\quad E=(-20-46x)W,$$
$$|\Gamma_5,1\rangle = 7^{1/2}2^{-1/2}2^{-1}|3\rangle - 2^{-1/2}2^{-1}|-1\rangle,$$
$$|\Gamma_5,0\rangle = 2^{-1/2}|2\rangle - 2^{-1/2}|-2\rangle,$$
$$|\Gamma_5,-1\rangle = 2^{-1/2}2^{-1}|1\rangle - 7^{1/2}2^{-1/2}2^{-1}|-3\rangle, \tag{5.4}$$

where we have written the wave functions in terms of the eigenfunctions of J^z. In Pr_3Tl the crystal-field approximates that of a fcc lattice and the value

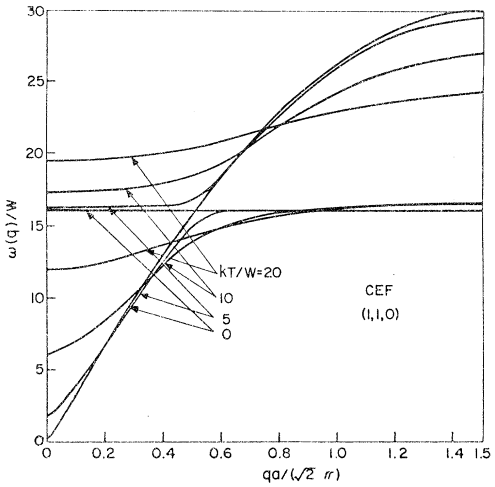

FIG. 10. As Fig. 9, but calculated in the CEF approximation.

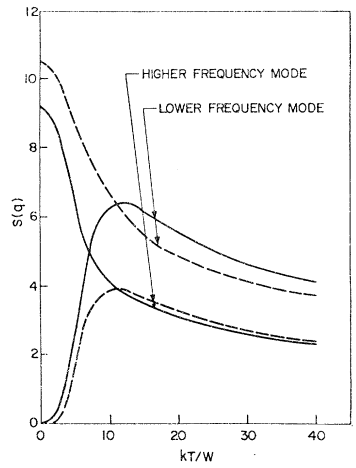

FIG. 12. Temperature variation of the scattering strengths of the two [110] modes of Figs. 9 and 10 at the wave vector $qa/\sqrt{2} = 0.554\pi$. Full curves represent the CEF approximation and dashed curves the RPA approximation.

of x is thought to be close to that predicted by a nearest-neighbor point-charge model, viz., $x = -0.877$. The resulting sequence of energy levels, and arrows representing the nonzero matrix elements of J^z between the eigenfunctions (5.1)–(5.4), are shown in Fig. 7.

In this section we shall concentrate on the differences between the CEF and RPA theories for dispersion and mode strength of the finite-frequency modes in this fcc $J=4$ model. For numerical computation we have chosen the exchange to be just sufficient to produce ferromagnetic order at $T_C = 0$, in which case the present theory can be applied at all temperatures. This can be achieved in Pr_3Tl by magnetic dilution of Pr with La to $(Pr_{0.93}La_{0.07})_3Tl$. Using the eigenstates (5.1)–(5.4) and their respective eigenvalues as the $|m\rangle$ and $|n\rangle$ and E_m and E_n of the theories of Secs. II and III we can immediately determine the matrix elements J^z_{mn} and in particular the ensemble average $\langle J^z : J^z \rangle_0$ of (2.10). Using (4.3) for the Curie temperature $T_C = 0$ gives

$$4\mathcal{J}(0)(1-\alpha_C) = \tfrac{3}{20}[E(\Gamma_4) - E(\Gamma_1)] = 3.392W \qquad (5.5)$$

as the value of "critical exchange" just necessary to produce ferromagnetism at absolute zero. With $\alpha_C = 0.256$ for nearest-neighbor-only fcc exchange in CEF (and $\alpha_C = 0$ in RPA) we again see that a larger exchange is predicted for the correlated theory. Using (2.8) we can now compute the complete temperature dependence of the correlation parameter in CEF; it is shown in Fig. 8.

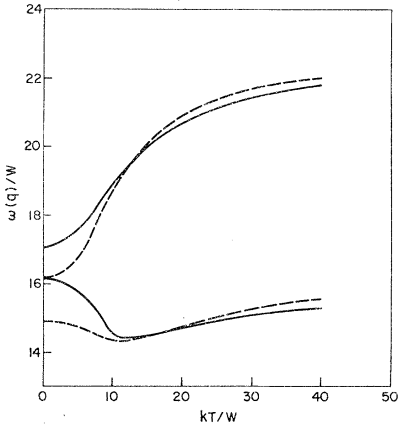

FIG. 11. Temperature variation of the frequencies of the two [110] modes of Figs. 9 and 10 at the wave vector $qa/\sqrt{2} = 0.554\pi$. Full curves represent the CEF approximation and dashed curves the RPA approximation.

Knowing the temperature dependence of α now allows a numerical solution of (3.16) to be obtained for the excitation frequencies. The zero-frequency terms do not contribute to the finite-frequency solutions. At the lowest temperatures only the Γ_1-Γ_4 excitation exhibits any dispersion. As the temperature is raised, however, a significant interaction develops between this mode and the Γ_4-Γ_3 mode as the latter becomes thermally populated. At temperatures up to $100W/k$, where $W \sim 3k$ in the Pr_3Tl system, little dispersion or mode strength develops for the higher-energy Γ_4-Γ_5 and Γ_3-Γ_5 modes and we shall concentrate here on the manner in which the lowest two finite-frequency modes develop and interact as a function of increasing temperature.

To be specific, we have computed the dispersions along a [110] direction in reciprocal space (a direction which has particular significance in connection with the Pr_3Tl structure proper[17]). The results for the RPA and CEF calculations are shown respec-

tively, in Figs. 9 and 10. The similarity of the two sets of curves is evident but two significant differences are apparent; one is the greater dispersion of the Γ_1-Γ_4 mode at low temperatures in CEF and the other the absence of a temperature-independent point in the CEF curves such as occurs at $qa = \sqrt{2}\,\pi$ in the RPA approximation (where a is cubic-unit-cell dimension in real space). Quantitative differences can be displayed more graphically by taking a representative wavelength, for which mode interaction is significant, and plotting the temperature development of the frequencies and the associated mode strengths [the latter calculated from (3.17)]. We have chosen the wavelength which for Pr_3Tl corresponds to 2 Å, viz., $qa/\sqrt{2} = 0.554\pi$, which satisfies the interaction criterion quite well (see Figs. 9 and 10). The computed temperature variations of frequency and strength for this [110] mode are shown in Figs. 11 and 12 where we display both the CEF and RPA estimates.

At low temperatures the scattering strength is dominantly in the Γ_1-Γ_4 mode; but this is the upper-frequency mode in CEF and the lower-frequency mode in RPA at this wavelength. As temperature is increased the mode strength in the Γ_4-Γ_3 mode rapidly increases and mode mixing becomes significant. In CEF the upper-frequency mode retains a dominantly Γ_1-Γ_4 character at all temperatures with mode strength decreasing monotonically with increasing temperature. The lower mode retains its dominant Γ_4-Γ_3 character throughout with mode strength passing through a maximum at intermediate temperatures. In RPA the lower-frequency mode is changed in character from Γ_1-Γ_4 to Γ_4-Γ_3 as the temperature increases, mode strength falling steadily. The upper-frequency mode in turn changes from Γ_4-Γ_3 to Γ_1-Γ_4 with strength passing through a maximum.

The important point is that the differences between the two approximations are often more than minor numerical deviations and it would be of considerable interest to compare each in turn with experiment. This will be attempted for the case of $(Pr_{0.93}La_{0.07})_3Tl$ in a future publication although one must bear in mind that neither approximation contains any measure of linewidth and that, as a result, both methods fall short of an adequate description of finite-temperature many-body dynamics in this more demanding sense. On the other hand, there should be some correspondence between experimental frequency response peaks and the frequencies and strengths discussed in this paper which might allow for some estimate of the relative strengths and weaknesses of the two approximations.

[1]M. E. Lines, Phys. Rev. B 9, 3927 (1974).
[2]R. Alben, Phys. Rev. 184, 495 (1969).
[3]M. E. Lines, Phys. Rev. B 9, 950 (1974).
[4]W. J. L. Buyers, T. M. Holden, E. C. Svensson, R. A. Cowley, and M. T. Hutchings, J. Phys. C 4, 2139 (1971).
[5]G. T. Trammell, Phys. Rev. 131, 932 (1963).
[6]B. Bleaney, Proc. R. Soc. Lond. A 276, 19 (1963).
[7]B. R. Cooper, Phys. Rev. 163, 444 (1963).
[8]B. Grover, Phys. Rev. 140, A1944 (1965).
[9]Y. L. Wang and B. R. Cooper, Phys. Rev. 172, 539 (1968); 185, 696 (1969).
[10]D. Pink, J. Phys. C 1, 1246 (1968).
[11]B. R. Rainford and J. Gylden Houmann, Phys. Rev. Lett. 26, 1254 (1971).
[12]R. J. Birgeneau, J. Als-Nielsen, and E. Bucher, Phys. Rev. Lett. 27, 1530 (1971); Phys. Rev. B 6, 2724 (1972).
[13]B. R. Cooper, Phys. Rev. B 6, 2730 (1972).
[14]Y. Y. Hsieh and M. Blume, Phys. Rev. B 6, 2684 (1972).
[15]S. R. P. Smith, J. Phys. C 5, L157 (1972).
[16]B. D. Rainford, AIP Conf. Proc. 5, 591 (1972).
[17]R. J. Birgeneau, AIP Conf. Proc. 10, 1664 (1973).
[18]Y. Y. Hsieh, Phys. Rev. B 8, 3459 (1973).
[19]R. Kubo, Rep. Prog. Phys. 29, 255 (1966).
[20]See, for example, V. L. Bonch-Bruevich and S. V. Tyablikov, *The Green's Function Method in Statistical Mechanics* (North Holland, Amsterdam, 1962), Sec. 14.
[21]T. M. Holden and W. J. L. Buyers, Phys. Rev. B 9, 3797 (1974).